Low-cost real-time fiber optic sensor for intrusion detection

Adel Abdallah
Department of Optoelectronics, Military Technical College, Cairo, Egypt
Mohamed M. Fouad
Department of Computer Engineering, Military Technical College, Cairo, Egypt, and
Hesham N. Ahmed
Department of Electronics Engineering, Military Technical College, Cairo, Egypt

Abstract

Purpose – The purpose of this paper is to introduce a novel intensity-modulated fiber optic sensor for real-time intrusion detection using a fiber-optic microbend sensor and an optical time-domain reflectometer (OTDR).

Design/methodology/approach – The proposed system is tested using different scenarios using person/car as intruders. Experiments are conducted in the lab and in the field. In the beginning, the OTDR trace is obtained and recorded as a reference signal without intrusion events. The second step is to capture the OTDR trace with intrusion events in one or multiple sectors. This measured signal is then compared to the reference signal and processed by matrix laboratory to determine the intruded sector. Information of the intrusion is displayed on an interactive screen implemented by Visual basic. The deformer is designed and implemented using SOLIDWORKS three-dimensional computer aided design Software.

Findings – The system is tested for intrusions by performing two experiments. The first experiment is performed for both persons (>50 kg) in the lab and cars in an open field with a car moving at 60 km/h using two optical fiber sectors of lengths 200 and 500 m. For test purposes, the deformer length used in the experiment is 2 m. The used signal processing technique in the first experiment has some limitations and its accuracy is 70% after measuring and recording 100 observations. To overcome these limitations, a second experiment with another technique of signal processing is performed.

Research limitations/implications – The system can perfectly display consecutive intrusions of the sectors, but in case of simultaneous intrusions of different sectors, which is difficult to take place in real situations, there will be the ambiguity of the number of intruders and the intruded sector. This will be addressed in future work. Suitable and stable laser power is required to get a suitable level of backscattered power. Optimization of the deformer is required to enhance the sensitivity and reliability of the sensor.

Practical implications – The proposed work enables us to benefit from the ease of implementation and the reduced cost of the intensity-modulated fiber optic sensors because it overcomes the constraints that prevent using the intensity-modulated fiber optic sensors for intrusion detection.

Originality/value – The proposed system is the first time long-range intensity-modulated fiber optic sensor for intrusion detection.

Keywords OTDR, Intrusion detection, Microbend sensor, Fiber-optic sensor, Perimeter security, Optical, Sensors

Paper type Research paper

1. Introduction

Nowadays, Terrorism, smuggling and acts of deliberate sabotage have become a threat to people's lives and economies of countries. Monitoring of perimeters and protection of important facilities play an important role in homeland security to avoid/mitigate these risks. Many researchers began to develop some systems for early warnings to face these threats. Some of these systems are based on fiber optic sensors (FOS) that have many advantages compared to conventional sensors (Giallorenzi *et al.*, 1982; Culshaw and Kersey, 2008). FOS are superior to their counterparts from geometry, size and weight points of view. These together with their robustness, large bandwidths and immunity to electromagnetic interference have motivated researchers to perform intensive work in this fruitful area.

Protecting borders and/or important facilities requires the ability to be deployed over long distances. This inherently requires developing high-performance yet relatively low-cost systems.

FOS can be classified into intensity, phase and wavelength-modulated FOS, in addition to polarization and scattering FOS (Krohn *et al.*, 2014). Intensity-type FOS generally depends on the changes of the output light intensity when the optical fiber is subjected to an external perturbation. It can be constructed based on microbending, reflection from a moveable reflector or evanescent wave coupling phenomenon. The major advantage of the microbend FOS over others is its simplicity, low cost and the ability to be combined with a conventional optical time-domain reflectometer (OTDR) to extend its capabilities and applications. The principle of microbend fiber-optic sensor was first proposed

The current issue and full text archive of this journal is available on Emerald Insight at: **https://www.emerald.com/insight/0260-2288.htm**

Sensor Review
© Emerald Publishing Limited [ISSN 0260-2288]
[DOI 10.1108/SR-03-2021-0090]

Military Technical College.

Received 15 March 2021
Revised 17 July 2021
Accepted 6 October 2021

in Fields *et al.* (1979). Since then these kinds of sensors were developed and have been used in many fields for measuring displacement, acoustic pressure, temperature, force, structural defects, vibration and for medical applications (Lagakos *et al.*, 1981, 1982; Lumholt *et al.*, 1991; Pandey and Yadav, 2007; Efendioglu *et al.*,2009; Garcia *et al.*, 2010; Lau *et al.*, 2013). The development process included the shape and design of the deformer (Morozov *et al.*, 2010) or even using other types of optical fibers like microstructured optical fibers to improve their performance (Borisov *et al.*, 2009). The mathematical models and the design parameters of the fiber-optic microbend sensors are discussed in Lagakos *et al.* (1987). The microbending effect has been considered in multimode fibers as a transduction mechanism for sensing environmental changes, such as pressure, temperature, acceleration and magnetic and electric fields (Lagakos *et al.*, 1987). A generic microbend sensor has been defined, studied and its components such as the sensing fiber, light source, optical fiber leads and detector have been examined, optimized and developed (Lagakos *et al.*, 1987; Donlagic and ZavrÏsnik, 1997; Wang *et al.*, 2012). The required system is used to secure important facilities to allow investigation or taking suitable action with trespassers of bad intentions. This requires using a system that can determine the sector and/or the distance to the threat. The microbend sensor needs to be combined with an OTDR to determine the distance to the event. The basic function of the OTDR is using the detected backscattered and the reflected light from connectors or cleaved fiber ends for testing the fiber optic cables. Using OTDR Based fiber-optic microbend sensor for sensing applications is proposed, for example, for structural pressure monitoring (Bino *et al.*, 2006). Some papers discussed intrusion detection using sophisticated techniques depending on measuring the points of phase changes using phase-OTDR (φ-OTDR) or polarization changes using polarization-OTDR (P-OTDR) due to the effect of intrusion. The principle of operation, design, implementation and development of φ-OTDR for intrusion detection are reported in Choi *et al.* (2003), Fang *et al.* (2015), Shi *et al.* (2015), Ren *et al.* (2016), Aktas *et al.* (2017), Muanenda *et al.* (2017), Peng *et al.* (2014), Juarez *et al.* (2005), while that of P-OTDR are reported in Linze *et al.* (2012), Hajj *et al.* (2015), Chen *et al.* (2018). Some advanced techniques are used to develop these systems and improve the localization mechanism are reported in Sun *et al.* (2015), Liu *et al.* (2018), Muanenda *et al.* (2018), Li *et al.* (2014), Franciscangelis *et al.* (2016), Muanenda (2018), Wang *et al.* (2017). Although these systems seem to perform well it requires complex design and expensive components for system realization [such as a spectrally stable narrow-linewidth laser source housed in a thermally insulated enclosure for low-frequency drift and single-mode fiber (Juarez *et al.*, 2005)] along with complex signal processing for classifying targets and reducing the false alarm. Furthermore, because these systems do not require direct pressure on the sensor, it is expected that because the sensor is very sensitive to vibrations the probability of false alarm will be high. On the other hand, the aim of this work is to propose a low-cost real-time fiber optic sensor that can be deployed long distances from an important facility for early warning against intrusions. The proposed intensity-type FOS based on measuring intensity changes uses cheaper components (such as LED or semiconductor laser with broad spectral width and multimode fiber), simpler signal processing and designed to respond to direct pressure immediately above the sensing fiber cable. The proposed sensor does not respond to weak vibrations from various environmental factors but it will respond to the real threats that attempt to approach the facility and this leads to reducing the false alarm to a large extent.

In this paper, the principle of microbend fiber-optic sensor is adopted for constructing the proposed intrusion detection system. Based on this study and the requirements, the most suitable system is a combination of a fiber optic microbend sensor and an OTDR. The microbend sensor attenuates light when subject to intrusion, while the OTDR determines the sector that has been breached or the distance to an intruder if it is required. Cost is an important factor so we used multimode optical fiber (MMF) and cheap deformer material with construction allows ease of manufacturing. The system is simple, cheap, accurate and can be deployed long-distance. One major advantage of the proposed system is that it can detect and monitor the sector subjects to intentional cut. While previously reported systems that use the idea of microbend FOS introduced a sensor with a short section which is not suitable for use as an intrusion detection sensor. This adds an advantage to the proposed system. The main drawback of the proposed system is that it cannot be used for the extraction of the acoustic signature of the intruder; instead, we depend on direct visualization or monitoring of the intruder by aiming the day/thermal camera at the intruded sector.

2. Proposed intrusion detection system

2.1 System modeling and simulation

The design of the proposed intensity-modulated fiber-optic sensor is based on bend-induced loss in an optical fiber that causes a change in the optical transmission through the bent optical fiber in response to an external effect. This leads to a change in the output signal of the photodetector and is used to detect the applied external effect. The structure of the sensor based on microbending loss, which was designed in the initial phase of this project, is shown in Figure 1. Intensity modulation induced by microbending depends mainly on the modal properties of the optical fiber and the construction of the deformer that converts the change in the external effect to an applied force on the bent optical fiber.

In our case, the amount of the change in the transmission coefficient for light propagating through the bent optical fiber can be calculated from (Lagakos *et al.*, 1987);

$$\Delta T = \frac{\Delta \mathrm{T}}{\Delta X}.\left(\frac{A_d Y_d}{l_d} + K_f\right)^{-1}.A_P.\Delta p \tag{1}$$

In which ΔX is the amount of the change in the amplitude of the fiber deformation in response to applied pressure, Δp is the change in the applied pressure, A_P is the area of the deformer plate, K_f is the force constant of the bent optical fiber, $\Delta T/\Delta X$ is the coefficient relates the change in transmission of light through the optical fiber to the change in the optical fiber deformation amplitude, l_d, A_d and Y_d are the length, the cross-section area and Young's modulus of the deformer spacers. Microbending loss is caused by coupling of the guided modes to radiated modes. As a result of the induced microbending along with the optical fiber, the power of the propagating is

Figure 1 The schematic of the sensor based on microbending loss using sensing MMF with deformer

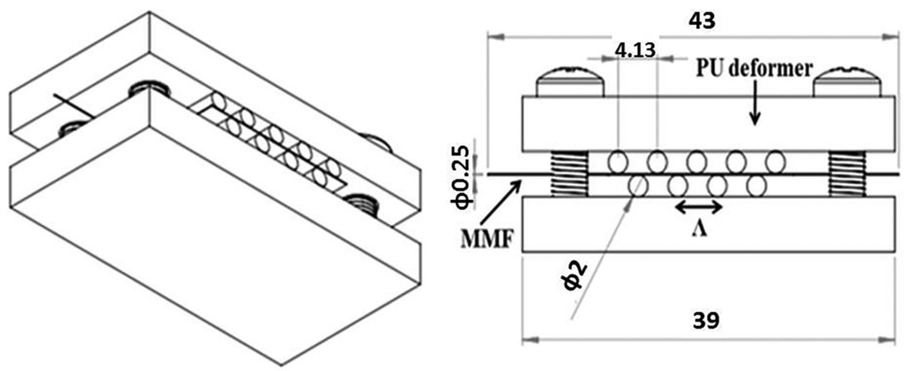

coupled between modes where the wavenumber separation of the neighboring modes for step-index fiber is expressed by:

$$K_{m+1} - K_m = \frac{2\sqrt{\Delta}}{r_c} \cdot \frac{m}{M} = \pm \frac{2\pi}{\Lambda} \tag{2}$$

Where $\Delta = (n_c - n_{cl})/n_c$ is fractional refractive index change, n_c is the core refractive index, n_{cl} is the cladding refractive index, r_c is the core radius, Λ is the mechanical periodicity of the deformer, m is the modal group label and M is the number of modal groups. The sensitivity of the sensor is enhanced when Λ is designed such that the microbending loss is due to the coupling of the highest guided mode to the first radiated mode. This critical mechanical periodicity is given by Lagakos *et al.* (1987);

$$\Lambda_c = \frac{\pi r_c}{\sqrt{\Delta}} \tag{3}$$

K_f is related to the deformer and the optical fiber parameters by;

$$K_f = \frac{3\pi\delta\, Y_f d_f^4}{\Lambda_c^3} \tag{4}$$

In which Y_f is the effective Young's modulus of the optical fiber, d_f is the diameter of the optical fiber δ is the number of the bending intervals.

2.2 Deformer design

The deformer design is crucial in microbend FOS. The deformer is mainly characterized by the used material, grooves' diameter/spacing and packaging that should be optimized to enhance the sensitivity of the system and allow it to be deployed long-distance. The proposed deformer used to perform the experiment consists of two parallel corrugated plates made of polyurethane with 2 m length, 2 cm width, 2.25 mm thickness and 2 mm mechanical periodicity as shown in Figure 2. The material and structure of this deformer achieve the cost and durability requirements. The experimental measurements showed that the material is solid enough but does not cause the optical fiber to break when subject to heavy loads like cars. Finally, the system is coated using rubber coating for protection, to increase the lifetime of the system and to prevent dust from gathering inside the grooves of the deformer.

2.3 Experimental setup

The proposed system block diagram is shown in Figure 3. The system consists mainly of seven major parts: the modulated laser source, a 1×2 directional coupler, a step-index MMF, avalanche photodetector (APD), the deformer, data acquisition and electronics and a computer for calculations, processing and display.

The laser source is a high-speed laser diode with a central wavelength of 868 nm. The used laser source can be controlled to produce pulse-width of 20 ns, 40 ns and 80 ns. In these systems, there is a tradeoff between spatial resolution and range. Narrower pulse width obtains better resolution but when the optical fiber length is increased, for example, to increase the number of sectors or the coverage area, the amplitude of the backscattered power is reduced; hence the S/N of the returned pulses is poor. In this experiment, the 80 ns pulse width was optimum enough by calculations and experiment to get reflected power with suitable amplitude and distinct peaks reflected from the ends of the sectors which is required to analyze the signals and determine the intruded sectors. In this case, the expected spatial resolution of the system is 8.25 m.

A laser diode is used in place of a LED to get proper reflected power from the ends of each sector and extend the range of the optical fiber to allow securing a longer distance. The 1×2 directional coupler module branches the reflected and backscattered light returned back from the fiber. The laser diode launches the light into one of the two arms and the APD detects the returning light energy from the other arm. The third arm on the opposite side of the coupler is used to connect the investigated optical fiber. Optical fiber spools are connected in series according to the required number of sectors and coverage area. The core, cladding and the acrylate coating diameters of the used MMF are 50 μm, 125 μm, 250 μm, respectively. Core/cladding materials are pure Silica/Fluorine-doped Silica. The NA of the optical fiber is 0.11, the refractive index of the core is 1.468 and the fractional refractive index change Δ = 0.0027. Based on these specifications and using equation (3), the calculated $\Lambda_c \approx 1.51$ mm. The realized deformer has Λ_c = 2 ± 0.1 mm. The maximum attenuation of the optical fiber at 850 nm is 5 dB/km and the scattering coefficient is -80 dB. The used connectors at the end of each sector are ST/PC Multimode connectors with Ceramic Ferrule. For test purposes, the deformer covers 2 m of one of the sectors of the proposed FOS which is the average width of most cars but in

Figure 2 Design of the proposed double-sided polyurethane deformer

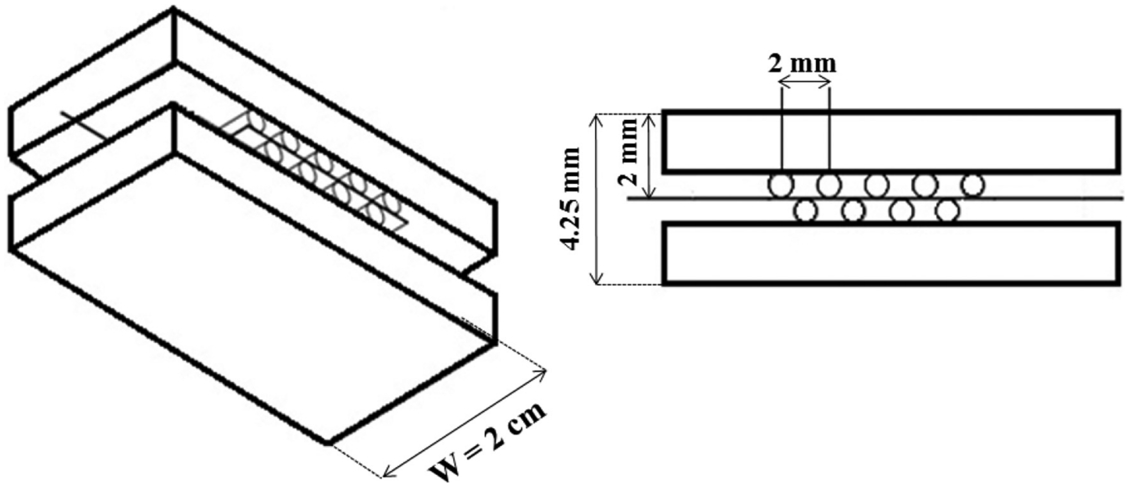

Figure 3 Proposed system block diagram

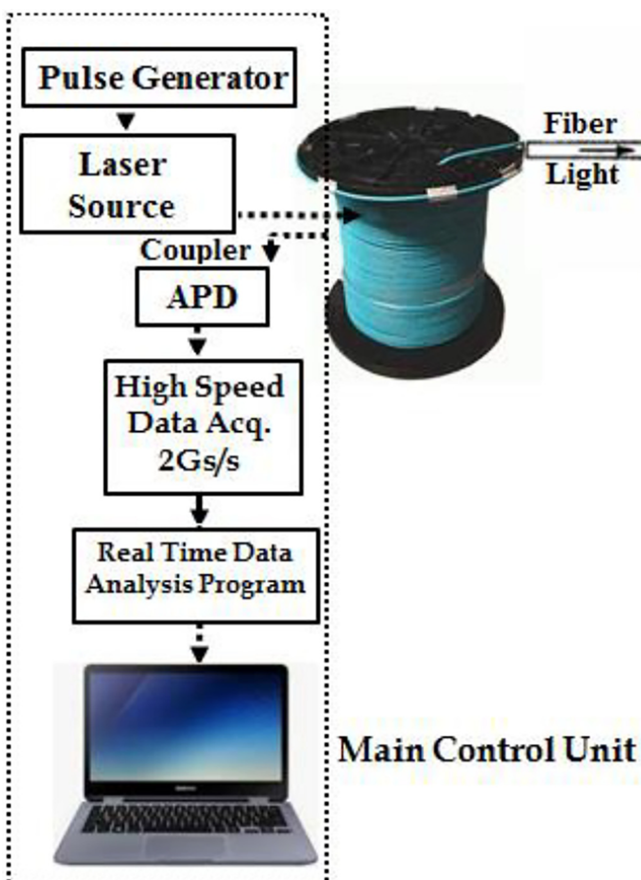

the case of deploying the FOS in its final state, the deformer covers the whole length of the optical fiber for proper operation of the sensor. A Silicon avalanche photodetector with a spectral range from 400 to 1,000 nm, the responsivity of 0.45 A/W at 850 nm and rise time 1 ns is used. Its output is connected to the oscilloscope through a Bayonet Neill-Concelman connector. The data acquisition system (DAQ) used is simply a 200-MHz Keysight Oscilloscope with a maximum sample rate of 2 GS/s. It is furthermore used for visualization and calibration of the system. It is connected to the computer for further processing, analysis and calculations using the developed code. All the above-mentioned parts of the system are within the premises of the protected entity with the fiber spools only being deployed. The first experimental setup of the system in the lab for testing the system functionally using two sectors is shown in Figure 4.

2.4 Principle of operation

Laser pulses of pulse width 80 ns and wavelength 868 nm are launched through the investigated MMF, sandwiched between upper and lower deformer, to attenuate the propagating signal when subjected to intrusion. The reflections from the reflective events and the backscattered light are received by an APD through a coupler, fed into a high-speed DAQ, analyzed and processed by a matrix laboratory code. In the beginning, the length and the numbers of sectors are determined. Optical fiber cables with end connectors are connected together to cover the area/building/borders to be secured. Each fiber cable represents a sector. Then we obtain and store a signature or a picture of the fiber link that has information on the events of the fiber at a specific time and environmental conditions. This is the reference signal that is used for comparison with the measured signals. For accurate results, in normal conditions, the reference signal is updated every 30 min to account for any environmental change. The amplitude of the reflected pulses at the end of each fiber is used to denote the sector such that when there is no intrusion the amplitudes of the reflected pulses from the end of each sector will remain the same and will not be attenuated, while if there is an intrusion at certain sector the reflected pulse will be attenuated and will be below a predetermined threshold. In this case, the proposed system can automatically identify the intruded sector. A camera is used to check the intruded sector, detect the intruder and track it. In the intruded sector, the date and time of intrusion are displayed in the control room on an interactive screen implemented by visual basic for proper decision as shown in Figure 5. In the figure, we have pentagon-shaped sectors but they can take any other shapes according to the required number/lengths of sectors.

2.5 Intrusion acquisition

Figure 6 shows the backscattered signal in case of no intrusion when using four sectors of optical fiber. The first pulse is the initial pulse due to the OTDR connector and the second pulse is the reflected pulse from the end of the first fiber section that represents the first sector and so does the remaining pulses. These returned pulses show the distances between the events (reflections from the ends of each fiber spool). The time difference between two successive peaks specifies an estimate for the length of the spool (sector length). Figure 7 shows the backscattered signal when sector 4 is intruded. It can be deduced that sector 4 is intruded because the reflected last pulse is diminished. A lead fiber, which is not coated with a deformer may be used to extend from the control room to the optical fiber of the first sector. The initial pulse is not taken into consideration because it does not represent any of the optical fiber sectors. This can be easily considered in the processing code.

3. Experimental results

In the beginning, the experiment is performed in the lab to test the system for person intrusions (>50 kg) using a single straight optical fiber but we cannot make sure that everyone who passes over the sensor will press it and will be detected as shown in Figure 8(a). To detect people we designed a zigzag-shaped optical fiber system based on a man's average step length which is approximately 31 inches (Extension, 2018). The overall length of the used fiber is about 200 m and covers a 50-meter sector as shown in Figure 8(b). We tested this sensor outdoor prior to performing the experiments for car intrusions. Although this design allows detecting people with a high degree of confidence, this comes at the expense of increasing the optical fiber length at each sector and consequently the cost of the system is increased. The proposed study focuses on vehicles detection using a single straight optical fiber as most terrorist attacks are carried out using them.

The sensor and the experimental components are moved to a yard near the car's garage to test it for cars intrusions. In the beginning, the experiment is performed using 700 m of optical

Figure 4 the first experimental setup in the lab

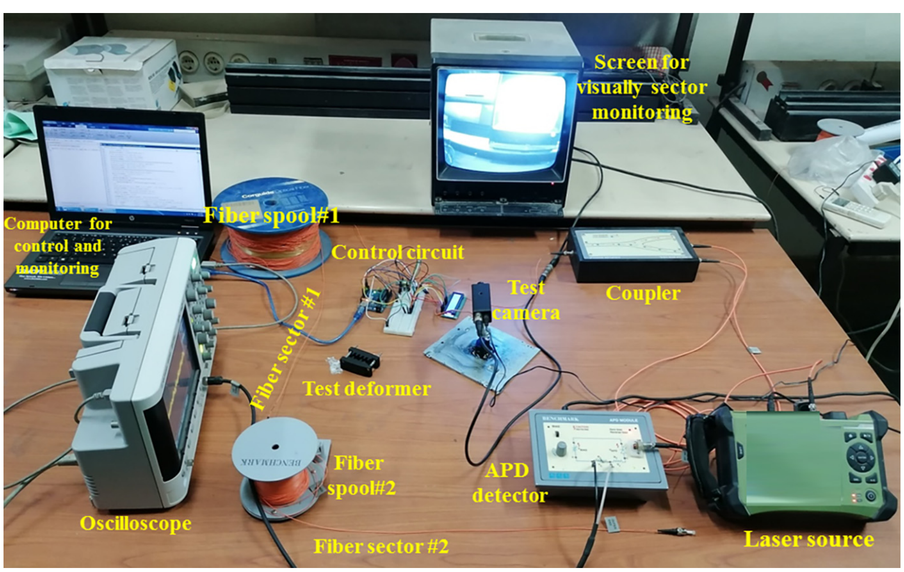

Figure 5 The interactive screen in the control room shows the locations and timing of the threats for proper decision

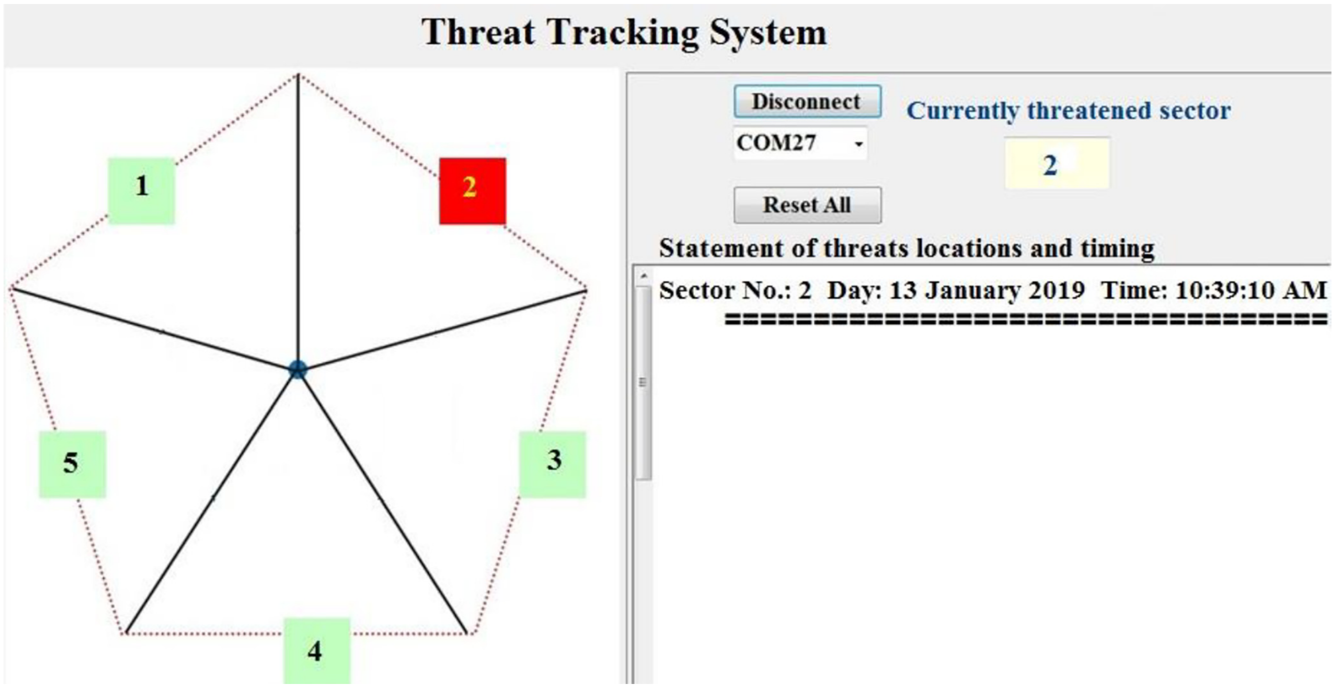

Figure 6 Backscattered signal when no intrusion

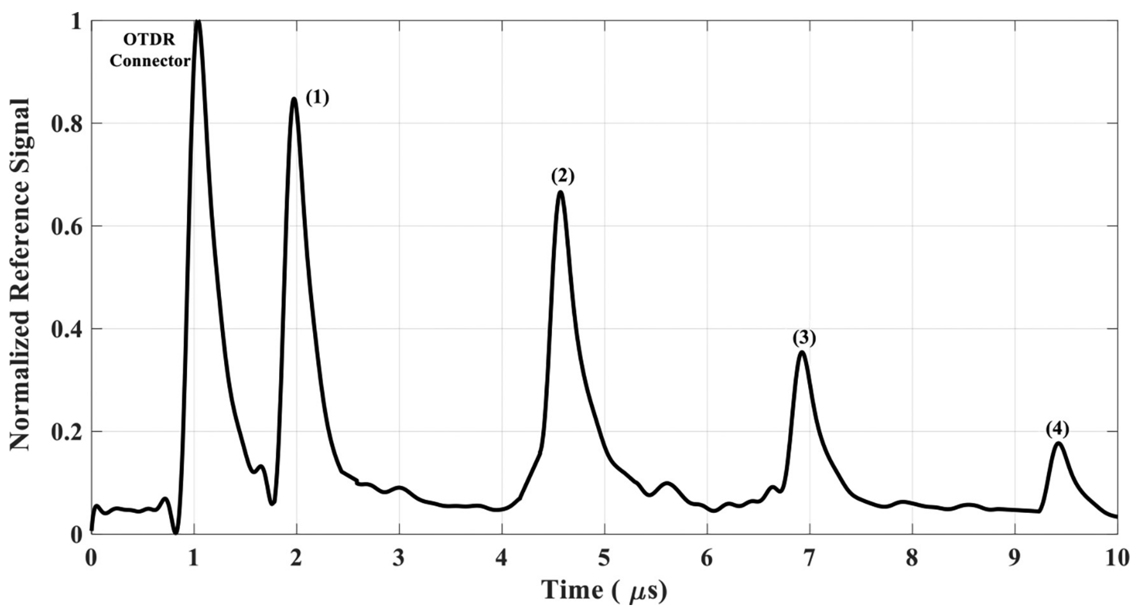

fiber, consists of two sectors: the first sector is represented by a 200 m length optical fiber spool while the second one is a 500 m spool. The used sample of the deformer length is 2 m. The second phase of the experiment is performed using 950 m of optical fiber consists of four sectors have lengths of 200 m, 300 m, 200 m and 250 m, respectively. For the cars test, although the heavyweight of the cars the optical fiber has not been cut. This shows that the structure and the chosen material of the deformer are suitable for our purpose.

The first task is to acquire the signal of the reflected and the backscattered light from the optical fiber link without intrusions and save it as a reference signal for later comparison with measured signals. For the used two sectors the reference signal is shown in Figure 9. The signal in the figure has three main peaks. The first peak represents the reflection from the connector of the laser source, while the second and the third peaks represent the reflections from the ends of the first and the second sectors, respectively.

Figure 7 Backscattered signal when sector 4 is intruded

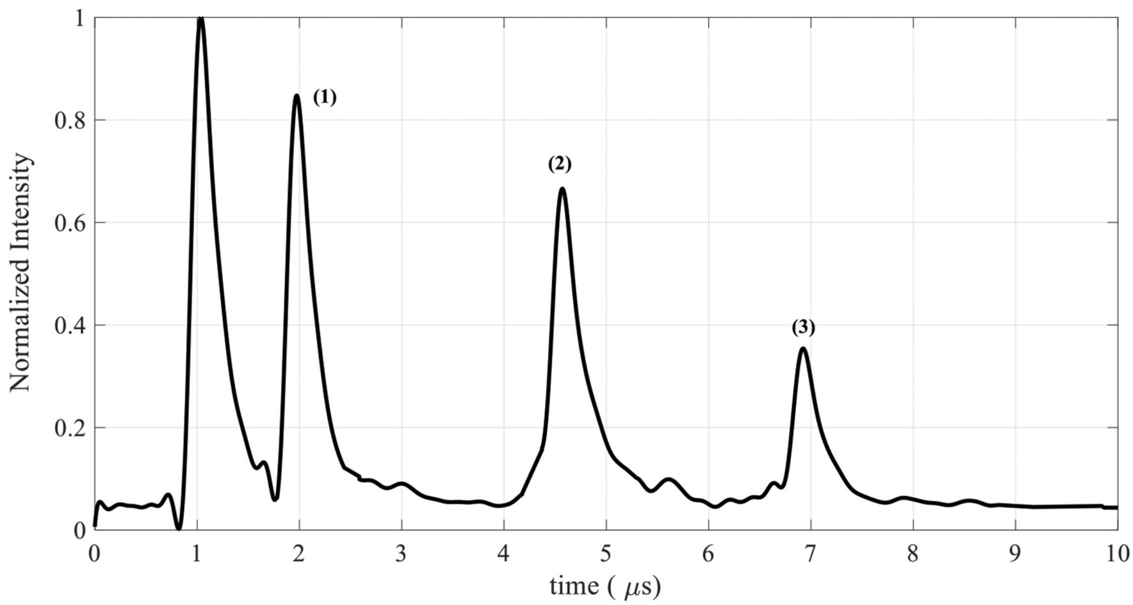

Figure 8 Sensor setup for detecting people

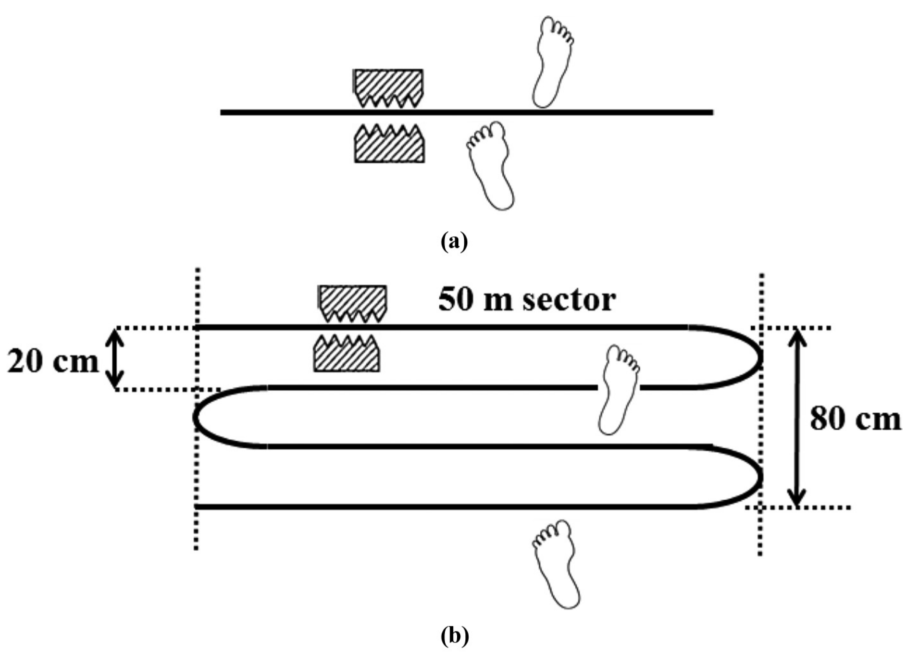

Notes: (a) Straight optical fiber; (b) Zigzag-shaped optical fiber

The second task is to operate the system in the search mode by continuously acquiring the signals using "while loop." The acquired signals are then measured signals to be compared with the recorded reference signal. Figure 10 shows a plot of the reference signal and the measured signal in case of no intrusions. It can be seen that without intrusions, the reference and the measured signals are almost identical. It can be seen that there are many ripples between the second and third peaks. For accurate calculations and to avoid the effect of these ripples, a threshold is determined such that the amplitude of the measured signal must be above this threshold to be considered. It is noticed that the reference signal and the measured signal are not perfectly matched, which can be attributed to the change of the environmental conditions during the day and the slight chance of the laser pulses amplitude. This is improved by normalization and updating the reference signal every 30 min.

One of the used techniques to determine the intruded sector is to calculate and plot the difference between both signals allow us to determine whether there are intrusions or not and to

Figure 9 The reference signal

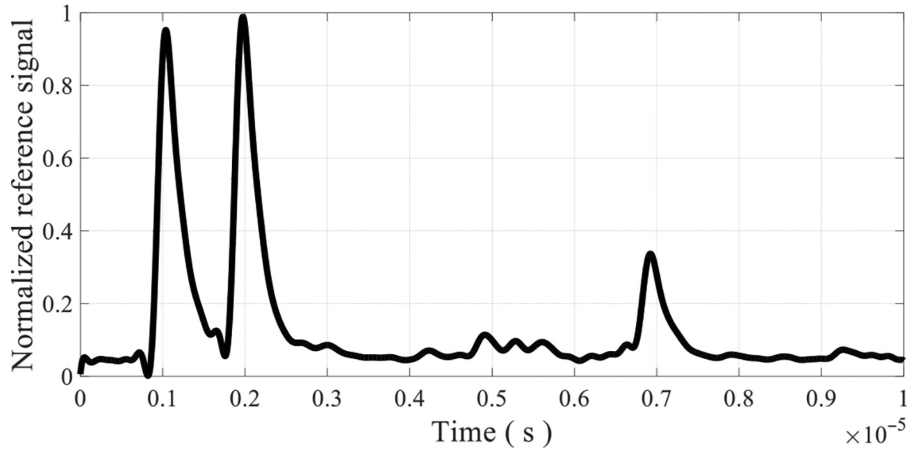

Figure 10 The reference signal and the measured signal in case of no intrusions

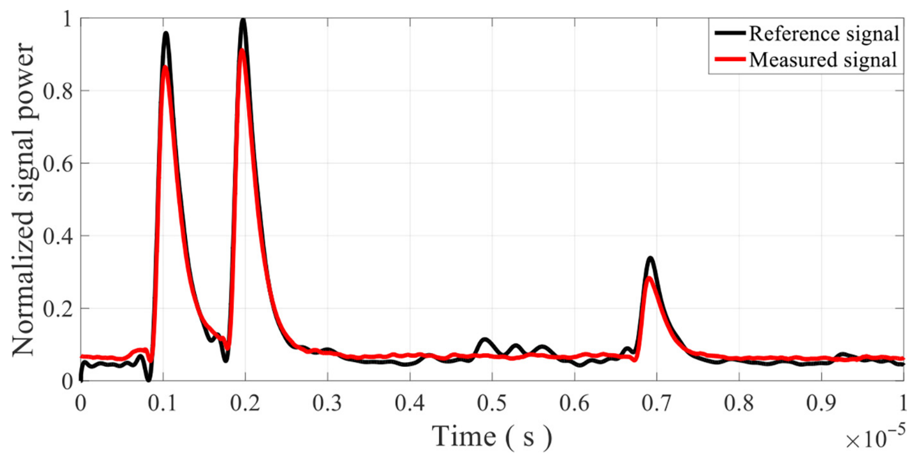

determine the intruded sector. The lag between the signals is calculated by the cross-correlation and used to align the reference and the measured signals and then the difference between both signals is calculated. Figure 11 shows the reference signal, the measured signal and the difference between them in case of no intrusions. It can be seen that the difference is almost zero indicating that there are no intrusions and consequently, no alarm. In this case, the system continues in search mode.

Figure 11 The reference signal, the measured signal and the difference between them in case of no intrusions

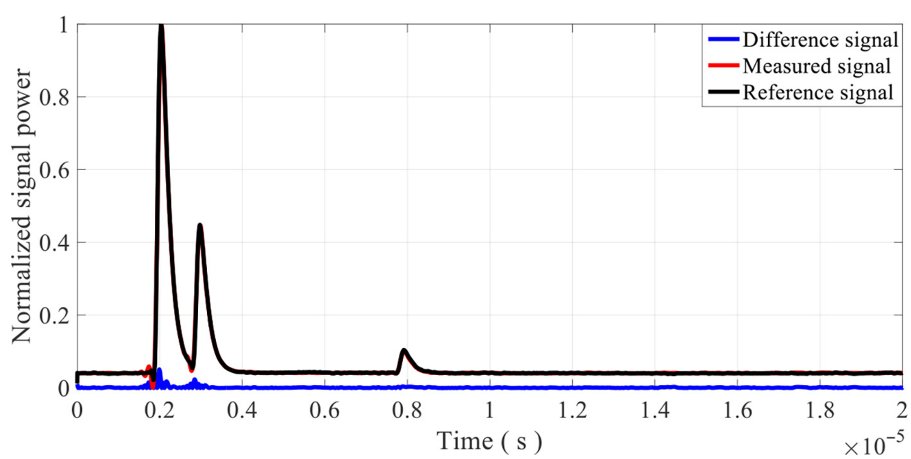

Figure 12 shows the reference signal and the measured signal when the system is tested using a car weighing 1.03 tons moving with a velocity of 60 km/hr. The car passed through the second sector, as a result, the amplitude of the reflected pulse energy from the end connector of the second sector of the measured signal is diminished compared to that of the reference signal.

Calculating the difference between both signals causes a peak to appear as shown in Figure 13. The peak with maximum amplitude determines the intruded sector. In this case, the intruded sector is determined, the alarm siren works and the intrusion information is displayed on the interactive screen on the control room as shown in Figure 5, Then the system continues the while loop searching for other intruders. It can be seen from the figure that there are unwanted peaks other than the required peak that represent the intruded sector. We needed to set a threshold and to choose the maximum peak to determine the right peak and consequently the intruded sector. This provides some uncertainty and measurement errors. To judge the performance of the system, 100 observations were measured and recorded. The success rate of the obtained results from this technique is about 70%.

Using the specifications of the system components and calculating the total rise time (t_r) of the introduced optical fiber sensor system (for the laser diode, the optical fiber due to different types of dispersion and the APD), it is found out that the total response time of the system is about 10 ns in the 700 m test range. As a result, although the experiment is performed at a relatively slow car speed (60 km/hr) due to the space limitations of the test area, the system is expected to respond effectively to all faster-intruded cars due to the fast response time of the system. The system response is very fast which is important to face threats, for example, if t_r of the system is about 10 ns, even if the car speed is 200 km/h and the optical fiber diameter is 250 μm which is the worst case (knowing that the used deformer width > 1 cm), the car will take time ≈ 4.5 μs > t_r.

The fixed length of the optical fiber and the fixed locations of the connectors at the end of the fiber allow getting a fixed time of the reflected pulses. This is exploited in the second phase of the experiment which is performed to overcome the limitations of the previous experiment. In this experiment, four optical fiber sectors and another technique of signal processing are used. The success rate and the reliability of the proposed system are improved by

Figure 12 The reference signal and the measured signal in case of using a car as an intruder

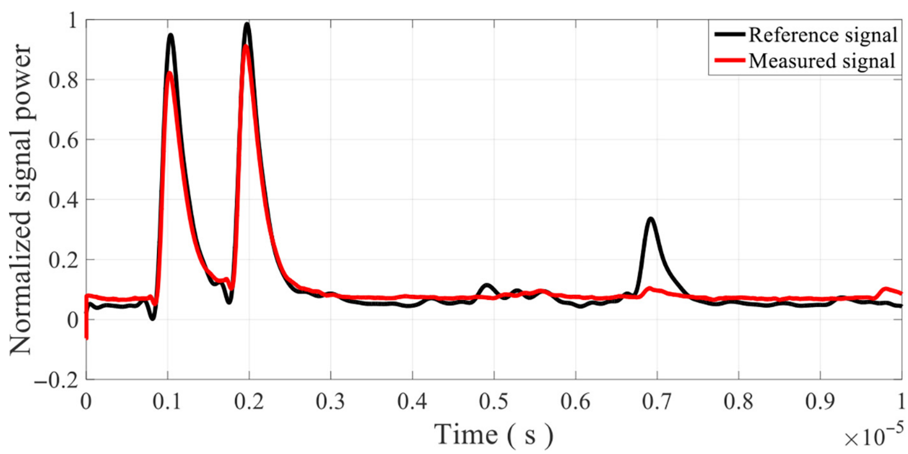

Figure 13 The reference signal and the difference signal in case of using a car as an intruder

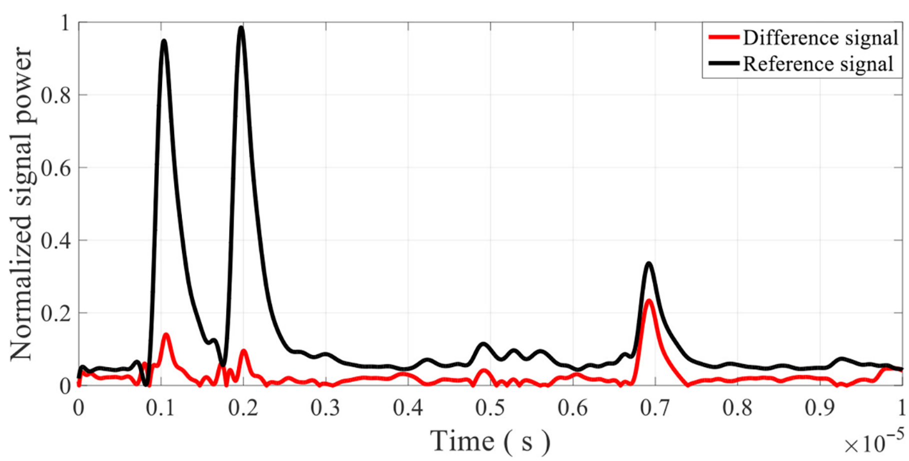

extraction of the signal level only in the specified time slots of the reflected pulses from the ends of the fiber sectors and comparing the intensity levels of the measured pulses to its corresponding reference pulses as shown in Figure 14. If the level of the reflected pulses from the sector ends is below a certain threshold level, this indicates that this sector is intruded. The threshold level is set for the individual pulse as shown in the figure. This technique allows avoiding the effect of the unwanted pulses and noise that appear in the time period between the successive pulses. After 100 observations using this technique, the probability of miss was zero and the intruded sectors were determined successfully.

The repeatability of the proposed sensor measurements is studied by observing the Rayleigh backscattering of the used optical fiber provided by the OTDR. The reflected amplitude of the same four fiber spools is measured using the same experimental setup once a week for six weeks relative to a stored reference signal. In this analysis, we measured the reflected amplitude of the reference signal and the six measured signals as shown in Figure 15 and the maximum normalized cross-correlation value as a method to test the repeatability of the measurements is calculated when the fourth sector is intruded and the car speed was 60 km/h. The same analysis can be

Figure 14 Comparing the levels of the reflected pulses of the measured signal with its corresponding reference signal reflected pulses from the four fiber sectors ends within the four-time slots

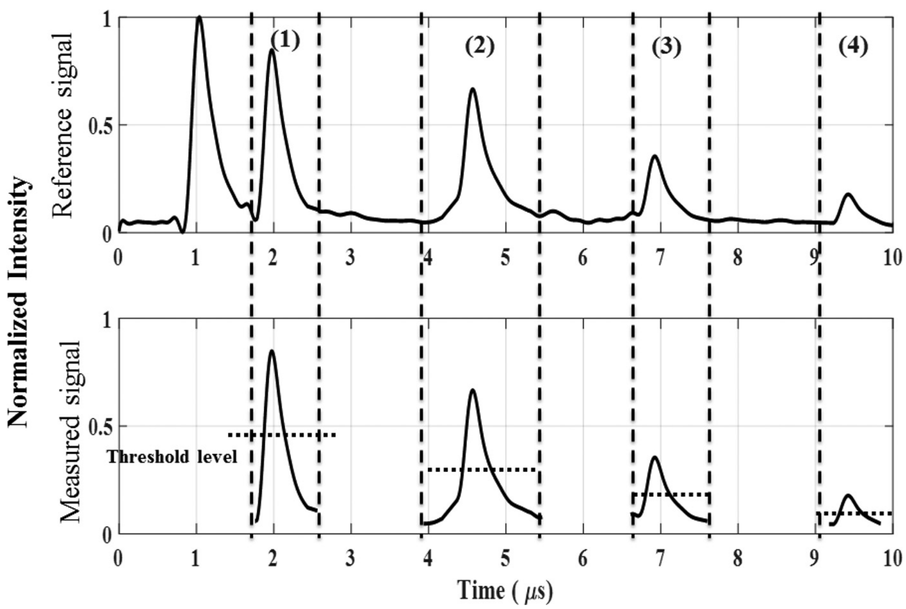

Figure 15 The reflected amplitude of the same four fiber spools measured six times when the fourth sector is intruded and the car speed was 60 km/h

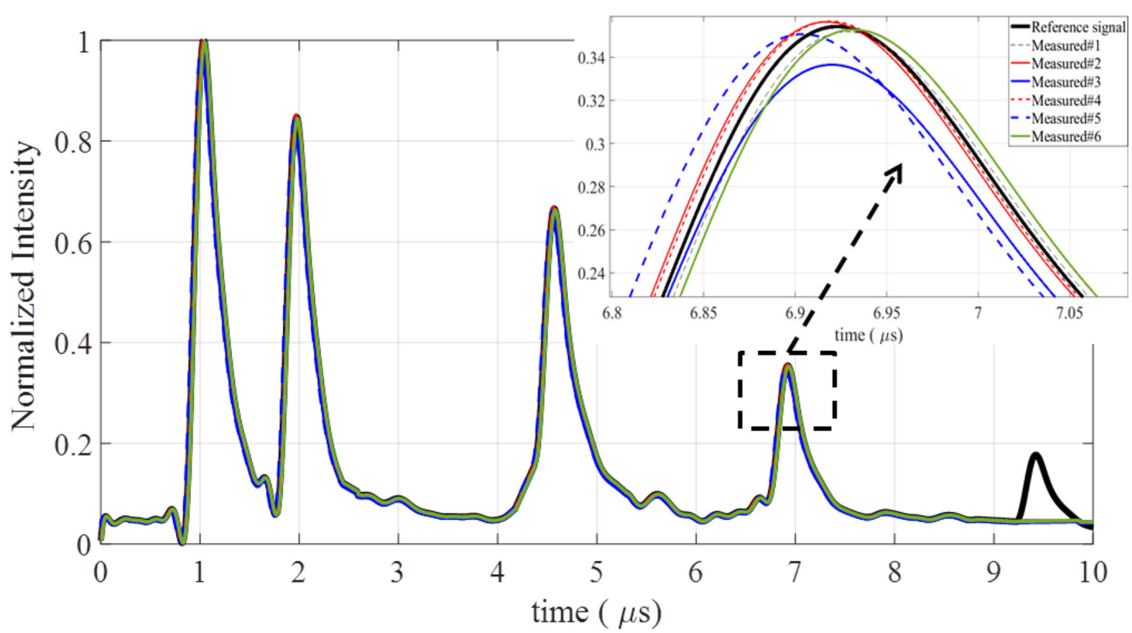

Algorithm 1: Proposed Algorithm for Intrusion Detection using Fiber Optic Microbend Sensor.

Input: Sampling rate, μ, Number of sectors, n, Reference signal, R, Threshold level, τ_{th}.
Output: Intruded Sector, S_i, while $1 \leq i \leq n$, and i denotes the sector index.
Steps:

1. Repeat
2. Measure the current signal (*i.e.*, measured signal), M.
3. Align the measured signal, M, to the reference signal, R, using correlation function by the equation, $XCOR_{RM}(\tau) = \frac{1}{T}\int_0^T R(t)M(t+\tau)dt$
4. Determine the set of reflected peaks of M ∀ n sectors, and denote their count as N_M.
5. Determine the number of reflected peaks of R; denoted by N_R.
6. Compute the magnitude of each reflected peak, P_i, of M.
7. Compute the magnitude of each reflected peak, L_i, of R.
8. if ($N_M = N_R$) AND ($P_i \equiv L_i$, ∀ i) then i = Φ; (*i.e.*, no intrusion)
9. else
10. Compute diff = $\sum_{i=1}^{n} |P_i - L_i|$,
11. if (diff > τ_{th})
12. Determine P_i, where P_i has the maximum magnitude
13. Display the corresponding S_i
14. end-if
15. end-if
16. until;

applied when other sectors are intruded on. The repeatability in the reflected amplitude of the six measurements can be seen and this confirms that the system is reliable.

The slight difference in the amplitudes and times of the peaks of the measured signal can be attributed to a tolerance of the optical power of the used laser diode and the temperature difference in the optical fiber when the measurements were recorded. A method to test the repeatability of the measurements is to calculate the similarity of the reference signal and the measured signals using normalized cross-correlation. Each of the six measured signals is compared to the reference signal and the maximum values of the normalized cross-correlation are calculated as shown in Table 1. The average matching level is 99.2% which is acceptable for our purpose.

The real-time detection algorithm for the proposed intrusion detection system is as follows:

Table 1 The calculated repeatability based on the maximum normalized cross-correlation value

Signal	Matching level
Reference	1
Measured#1	0.9972
Measured#2	0.987
Measured#3	0.991
Measured#4	0.985
Measured#5	0.995
Measured#6	0.989
Average matching	*0.992*

4. Conclusion

In this paper, real-time intrusion detection using a fiber-optic microbend sensor and an optical time-domain reflectometer (OTDR) is proposed and experimentally demonstrated. The simple, cost-effective (compared to other optical fiber sensing techniques) proposed system can detect intrusions in real-time with high sensitivity. The system is tested for intrusions of both persons (>50 kg) in the lab and cars in an open field with a car moving at 60 km/hr in a 700 m test range comprising two sectors of lengths 200 and 500 m, respectively. The deformer length used in the experiment is 2 m. The experimental results in the case of the presence of intrusions and without intrusions are shown and discussed. In case of intrusion, the sector is determined, a visible and audible alarm system works and the intrusion information is displayed on the interactive screen in the control room. A second experiment is performed using four optical fiber sectors using another technique of signal processing to improve the performance of the system and to overcome some limitations in the first experiment. To measure the repeatability of the measurements we measured the reflected amplitude of the reference signal and the six measured signals and the maximum normalized cross-correlation value is calculated when the fourth sector is intruded and the car speed was 60 km/h. The average matching level is 99.2% which is acceptable for our purpose. Finally, the real-time detection algorithm for the proposed intrusion detection system is introduced. The system can be simply modified to secure borders/important facilities with any requirements regarding length and number of sectors. This type of sensor depends on measuring the intensity level of the propagating light. The proper operation of the proposed optical fiber sensor requires a certain level of laser power depending on the total length of the sectors. This is to make sure that the reflected laser pulses from the ends of all-optical fiber sectors are above the certain threshold which was set to avoid the effect of the unwanted peaks between the fiber sectors.

References

Aktas, M., Akgun, T., Demircin, M.U. and Buyukaydin, D. (2017), "Deep learning based multi-threat classication for Phase-OTDR fiber optic distributed acoustic sensing applications", *Fiber Optic Sensors and Applications*, p. 102080G.

Bino, S., Pillai, V.P.M. and Chandrasekaran, N. (2006), "OTDR based fiber optic microbend sensor for distributed sensing applications in structural pressure monitoring", *Journal of Optics*, Vol. 35 No. 1, pp. 36-44.

Borisov, V.I., Minkovich, V.P. and Shilova, I.V. (2009), "Comparative analysis of classical and special single-mode microstructured optical fibers as a sensing element for fiber optic microbend sensors", *Optical Engineering*, Vol. 48 No. 5, p. 055006.

Chen, M., Chen, M., Wang, F., Wang, F., Zhang, Y., Zhang, Y., Zhang, X. and Zhang, X. (2018), "Measurement of multiple vibration points by using POTDR", *International Conference on Optical Instruments and Technology: Advanced Optical Sensors and Applications*, p. 1061803.

Choi, K.N., Juarez, J.C. and Taylor, H.F. (2003), "Distributed fiber-optic pressure/seismic sensor for low-cost monitoring of long perimeters", *Unattended Ground Sensor Technologies and Applications V*, pp. 134-141.

Culshaw, B. and Kersey, A. (2008), "Fiber-optic sensing: a historical perspective", *Journal of Lightwave Technology*, Vol. 26 No. 9, pp. 1064-1078.

Donlagic, D. and ZavrÏsnik, M. (1997), "Fiber-optic microbend sensor structure", *Optics Letters*, Vol. 22, pp. 837-839.

Efendioglu, H.S., Yildirim, T. and Fidanboylu, K. (2009), "Prediction of force measurements of a microbend sensor based on an artificial neural network", *Sensors*, Vol. 9 No. 9, pp. 7167-7176.

Extension, A.S.U. (2018), "The average walking stride length", available at: https://livehealthy.chron.com/determine-stride-pedometer-height-weight-4518.html

Fang, G., Xu, T., Feng, S. and Li, F. (2015), "Phase-sensitive optical time domain reflectometer based on phase generated carrier algorithm", *Journal of Lightwave Technology*, Vol. 33 No. 13, pp. 1-7.

Fields, J.N., Smith, C.P., Asawa, C.K., Morrison, R.J., Ramer, G., Tangonan, G.L. and Barnoski, M.K. (1979), "Multimode optical-fiber loss modulation acoustic sensor", *Technical Digest on Optical Fiber Communication*, Washington, DC.

Franciscangelis, C., Margulis, W., Kjellberg, L., Soderquist, I. and Fruett, F. (2016), "Real-time distributed fiber microphone based on phase-OTDR", *Optical Society of America*, Vol. 24 No. 26, pp. 29597-29602.

Garcia, Y.R., Corres, J.M. and Goicoechea, J. (2010), "Vibration detection using optical fiber sensors", *Journal of Sensors*, Vol. 2010.

Giallorenzi, T.G., Bucaro, J.A., Dandridge, A., Sigel, G.H., Cole, J.H., Rkshleigh, S.C. and Priest, R.G. (1982), "Optical fiber sensor technology", *IEEE Journal of Quantum Electronics*, Vol. 18 No. 4, pp. 626-665.

Hajj, R.E., MacDonald, G., Verma, P. and Huck, R. (2015), "Implementing and testing a fiber-optic polarization-based intrusion detection system", *Optical Engineering*, Vol. 54 No. 9, p. 096107.

Juarez, J.C., Maier, E.W., Choi, K.N. and Taylor, H.F. (2005), "Distributed fiber-optic intrusion sensor system", *Journal of Lightwave Technology*, Vol. 23 No. 6, pp. 2081-2087.

Krohn, D.A., MacDougall, T.W. and Mendez, A. (2014), *Fiber Optic Sensors: Fundamentals and Applications*, 4th ed., SPIE Digital Library, Bellingham, Washington, DC.

Lagakos, N., Cole, J.H. and Bucaro, J.A. (1987), "Microbend fiber-optic sensor", *Applied Optics*, Vol. 26 No. 11, pp. 2171-2180.

Lagakos, N., Litovitz, T., Macedo, P., Mohr, R. and Meister, R. (1981), "Multimode optical fiber displacement sensor", *Applied Optics*, Vol. 20 No. 2, pp. 167-168.

Lagakos, N., Trott, W.J., Hickman, T.R., Cole, J.H. and Bucaro, J.A. (1982), "Microbend fiber-optic sensor as extended hydrophone", *IEEE Journal of Quantum Electronics*, Vol. 18 No. 10, pp. 1633-1638.

Lau, D., Chen, Z., Teo, J.T., Ng, S.H., Rumpel, H., Lian, Y., Yang, H. and Kei, P.L. (2013), "Intensity-modulated microbend fiber optic sensor for respiratory monitoring and gating during MRI", *IEEE Transactions on Biomedical Engineering*, Vol. 60 No. 9, pp. 2655-2662.

Li, Q., Zhang, C., Li, L. and Zhong, X. (2014), "Localization mechanisms and location methods of the disturbance sensor based on phase-sensitive OTDR", *Optik*, Vol. 125 No. 9, pp. 2099-2103.

Linze, N., Mégret, P. and Wuilpart, M. (2012), "Development of an intrusion sensor based on a polarization-OTDR system", *IEEE Sensors Journal*, Vol. 12 No. 10, pp. 3005-3009.

Liu, X., Wang, Y., Wu, R., Wang, D., Bai, Q. and Jin, B. (2018), "Real-time phase-sensitive OTDR based on data matrix matching method", *Sensors*, Vol. 18 No. 6, p. 1883.

Lumholt, O., Bjarklev, A., Dahl-Petersen, S., Larsen, C.C., Povlsen, J.H., Rasmussen, T. and Rottwitt, K. (1991), "Simple fiber-optic low-temperature sensor that uses microbending loss", *Optics Letters*, Vol. 16 No. 17, pp. 1355-1357.

Morozov, O.G., Alekseev, A.N. and Pol'skii, Y.E. (2010), "Sensor on the twisted fibers for building constructions monitoring", *Optical Technologies for Telecommunications*, p. 75230J.

Muanenda, Y. (2018), "Recent advances in distributed acoustic sensing based on phase-sensitive optical time domain reflectometry", *Journal of Sensors*, Vol. 2018.

Muanenda, Y., Faralli, S., Oton, C.J. and Pasquale, F.D. (2018), "Stable dynamic phase demodulation in a DAS based on double-pulse ϕ-OTDR using homodyne demodulation and direct detection", *Fiber Optic Sensors and Applications*, p. 106540B.

Muanenda, Y., Oton, C.J., Faralli, S. and Pasquale, F.D. (2017), "A ϕ-OTDR sensor for high-frequency distributed vibration measurements with minimal post-processing", *presented at the 19th Italian National Conference on Photonic Technologies (Fotonica 2017)*, Padua.

Pandey, N.K. and Yadav, B.C. (2007), "Fibre optic pressure sensor and monitoring of structural defects", *Optica Applicata*, Vol. 37 Nos 1/2, pp. 57-63.

Peng, F., Wu, H., Jia, X.H., Rao, Y.J., Wang, Z.N. and Peng, Z.P. (2014), "Ultra-long high-sensitivity Φ-OTDR for high spatial resolution intrusion detection of pipelines", *Optics Express*, Vol. 22 No. 11, pp. 13804-13810.

Ren, M., Lu, P., Chen, L. and Bao, X. (2016), "Study of Φ-OTDR stability for dynamic strain measurement in piezoelectric vibration", *Photonic Sensors*, Vol. 6 No. 3, pp. 199-208.

Shi, Y., Feng, H. and Zeng, Z. (2015), "A long distance phase-sensitive optical time domain reflectometer with simple structure and high locating accuracy", *Sensors*, Vol. 15 No. 9, pp. 21957-21970.

Sun, Q., Feng, H., Yan, X. and Zeng, Z. (2015), "Recognition of a phase-sensitivity OTDR sensing system based on morphologic feature extraction", *Sensors*, Vol. 15 No. 7, pp. 15179-15197.

Wang, Z., Jiang, M., Xu, H. and Du, R. (2012), "New optical fiber micro-bend pressure sensors based on fiber-loop ringdown", *Procedia Engineering*, Vol. 29, pp. 4234-4238.

Wang, X., Chaodong, W., Tang, M., Fu, S. and Shum, P. (2017), "Multiplexed polarization OTDR system with high DOP and ability of multi-event detection", *Applied Optics*, Vol. 56 No. 13, pp. 3709-3713.

Corresponding author

Adel Abdallah can be contacted at: adel.abdallah@mtc.edu.eg